

OPTIMAL FOCUSING FOR LINAC-BASED HARD X-RAY SOURCE*

C. Liu[#], BNL, Upton, NY, U.S.A., R. Talman, Cornell University, Ithaca, NY, U.S.A., G. Krafft, TJNAF, Newport News, VA, U.S.A.

Abstract

In spite of having a small average beam current limit, a linac can have features that make it attractive as an x-ray source: high energy, ultralow emittance and energy spread, and flexible beamline optics. Unlike a storage ring, in which an (undulator) radiation source is necessarily short and positioned at an electron beam waist, in a linac the undulator can be long and the electron beam can be adjusted to have a (virtual) waist far downstream toward the x-ray target. Using a planned CEBAF beamline as an example, this paper shows that a factor of 2000 in beam current can be overcome to produce a monochromatic hard x-ray source comparable with, or even exceeding, the performance of an x-ray line at a third generation storage ring. Optimal electron beam focusing conditions for x-ray flux density and brilliance are derived, and are verified by simulations using the SRW code.

INTRODUCTION

There has been interest in developing linac-based x-ray sources since the success of the recirculating superconducting linac at the Thomas Jefferson National Accelerator Facility [1-4]. In [5], it has been elaborated that linac-based (with virtual electron beam waist at experiment target) hard x-ray beam can be superior or at least comparable to existing storage ring beams in terms of brilliance and flux density. Following the same scheme, this paper pursues how to optimize the flux density of a linac-based x-ray source by matching the optics.

PRINCIPLES

Due to the flexibility of optics in linac-based x-ray source, the waist-at-target scheme (focusing virtual waist of electron beam at experimental target instead of real electron beam waist in the middle of undulator in storage ring case) can enhance radiation flux density. The optimal focusing for maximizing flux density to be presented is based on the waist-at-target scheme. In the following analysis, we assume a helical undulator with length L_w , followed by a drift space L and an experimental target. The virtual waist of electron beam (the waist if the electron beam were not deflected by a bending magnet) is centered on the target. By concatenating the two inverted matrices of undulator and drift space, one obtains the following input Twiss functions:

$$= \begin{pmatrix} -\sqrt{K} \sin(2u)\beta/2 + \frac{1}{\beta} \left(\cos(2u)L - \sqrt{K} \sin(2u)L^2/2 + \sin(2u)/2\sqrt{K} \right) \\ \cos(u)^2 \beta + \frac{1}{\beta} \left(\cos(u)^2 L^2 + \sin(u)^2/K + \sin(2u)L/\sqrt{K} \right) \\ K \sin(u)^2 \beta + \frac{1}{\beta} \left(\cos(u)^2 + K \sin(u)^2 L^2 - \sin(2u)L/\sqrt{K} \right) \end{pmatrix} \quad (1)$$

K is the focusing strength of the helical undulator in both planes, u is the phase advance through the undulator, β is the virtual beta function of the electron beam at the target. The input beta function (the second element in Eq. 1), which depends only on the virtual beta function for a fixed beam line configuration, has a minimal value. The target value of input beta function is chosen to be close and somewhat higher than the minimum in [5], which will be named as min-input-beta case in this paper.

Consider electrons radiating at an arbitrary position z in the undulator (origin is at its entrance), the electron Twiss parameters at this position can be derived by propagating the Twiss parameters in Eq. 1 from undulator entrance to position z . The radiated photons inherit Twiss parameters of the electrons and drift all the way onto the target. The evolution of beta and gamma comply with

$$\beta_\gamma(z) = \beta(z) - 2\alpha(z) * (L_w + L - z) + \gamma(z) * (L_w + L - z)^2 \quad (2)$$

and

$$\gamma_\gamma(z) = \gamma(z) \quad (3)$$

Where, $\alpha(z)$, $\beta(z)$ and $\gamma(z)$ are the electron beam Twiss parameters at position z in the undulator and $\beta_\gamma(z)$ is the beta function of photon beam at target. As in [6], the standard deviation of emittance-determined x-ray spot size and divergence at target are proportional to average values of beta and gamma.

The following calculation is based on 50 m long helical undulator, with 16 mm period and undulator strength 0.687. In order to optimize flux density, one needs to minimize the averaged beta function in Eq. 2. Together with input electron beam beta function, the average of x-ray beta function is plotted in Fig. 1 showing the dependence on virtual beta function at target. The min-input-beta case, which corresponds to the minimum of electron beam input beta function curve (dashed line), is basically an attempt to keep both x-ray spot size and input electron beam size relatively small. However, the minimum of average x-ray beta function curve (solid line), which will be named as min-xray-spot, tries to minimize the x-ray spot size by permitting increased beta function at the undulator entrance. Fortunately, the beta

*The work was performed under Contract No. DE-AC02-98CH10886 with the U.S. Department of Energy.

[#]cliu1@bnl.gov

function at the entrance of undulator remains acceptable; corresponding to the minimum of the solid curve, it is around 300 m, which is a value well achievable by optical matching.

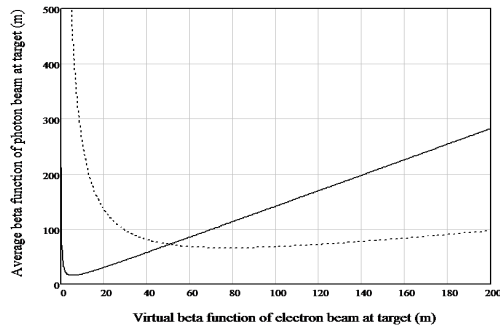


Fig. 1: Average beta function of photon beam at target (solid line), electron beam input beta function (dashed line) versus virtual beta function of electron beam at target

Similar analysis also applies to an x-ray beam produced from a planar undulator, requiring only separate treatment of the focusing in two transversal planes. An alternative method of optimization is under study as well, the basic idea of which is to start from Twiss parameters at entrance of undulator instead of at target.

SRW CALCULATIONS

To verify the idea of optimal focusing for a linac-based x-ray source, SRW simulations [7] have been carried out for ESRF and the proposed CEBAF x-ray beam lines. The electron beam and undulator parameters of both machines are listed in Table 1.

Table 1: Beam and undulator parameters for hard x-ray source at ESRF and CEBAF

Parameters	Unit	ESRF ideal helical	CEBAF long helical	
			Min-input-beta	Min-xray-spot
Undulator length	m	5	50	
Undulator period	mm	16	16	
Undulator strength		0.687	0.687	
Drift length	m	55	10	
Beam energy	GeV	8	8	
Average current	mA	200	0.1	
Beam emittance	nm	3.9/0.039	0.035	
Photon energy	keV	26	26	
Input alpha		1.79/0.312	0.1	2.546
Input beta	m	3.68/4.52	72.305	259.743
Input gama	1/m	1.43/0.25	0.014	0.0288

The flux density curves for ESRF and CEBAF are plotted in Fig. 2-3; and flux density with optimal focusing for CEBAF is shown in Fig. 4. As we can see, the long undulator alone could not compensate the disadvantage of current (factor of 2000) at CEBAF; with taking into account the spot size advantage due to low emittance, the flux density of CEBAF is still a factor of 2 lower than that of ESRF. The comparable results in Fig. 2 & 3 are attributable to the waist-at-target scheme. The higher flux density in Fig. 4 is the result of optimal focusing which not only puts virtual electron beam waist at target but also minimizes the x-ray spot at target. The improvement due to optimal focusing is a factor of 2 increase of flux density. The relative bandwidth for CEBAF is also much narrower (1/15) than that of ESRF, which provides natural quasi-monochromatic x-ray beam. Furthermore, the relative bandwidth is reduced to half with the optimal focusing in Fig. 4. Together with the fact that radiation from helical undulator is mostly fundamental, a beam line without monochromator is possible for a high energy linac-based x-ray source.

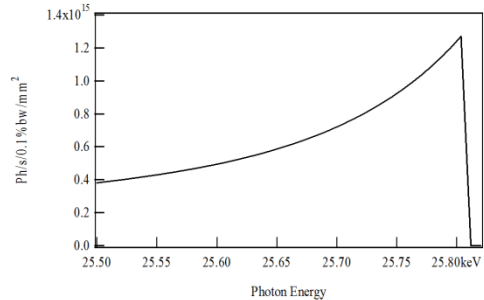


Fig. 2: Energy dependency of flux density for ESRF

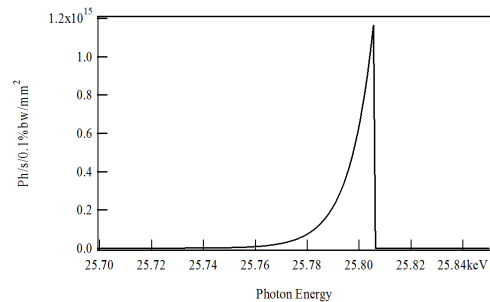


Fig. 3: Energy dependency of flux density for min input case at CEBAF

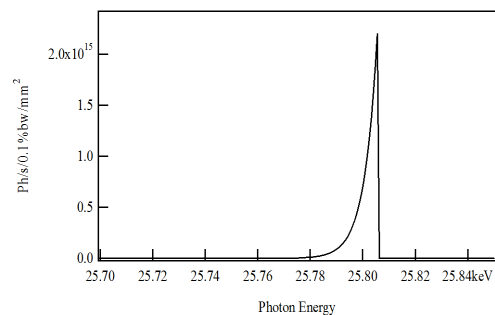


Fig. 4: Energy dependency of flux density for min x-ray spot case at CEBAF

Two dimensional intensity distributions of on-momentum x-rays for ESRF are displayed in Fig. 5; both on- and off-momentum x-ray intensity distributions for CEBAF are shown in Fig. 6, and Fig. 7, which is the case with optimal focusing. Note the sharper images for the min-x-ray-spot case.

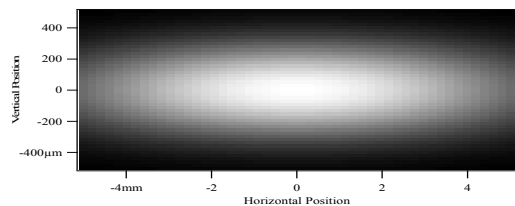


Fig. 5: Intensity distribution of on-momentum x-ray for ESRF

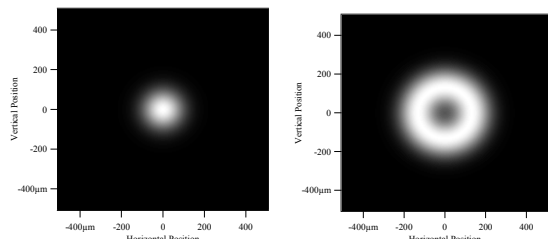


Fig. 6: Intensity distribution of on- and off-momentum x-ray for min-input-beta case

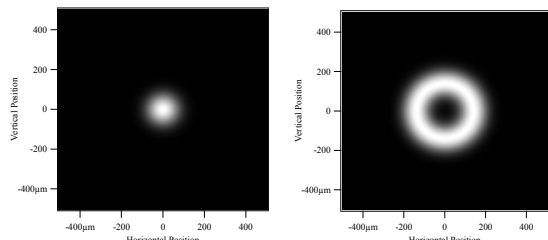


Fig. 7: Intensity distribution of on- and off-momentum x-ray for min-x-ray-spot case

The brilliance scales linearly with undulator length; therefore, longer undulator (factor of 10) and smaller emittance (factor of 100) for CEBAF enhance the brilliance by factor of 1000. Considering the lower current at CEBAF, a factor of ~2 difference of brilliance is expected for two facilities, which is confirmed by the results in Fig. 8 and 9. With decreasing x-ray spot size, the angular divergence increases, consistent with phase space density conservation. This explains why the brilliance in Fig. 10 drops comparing to Fig. 9.

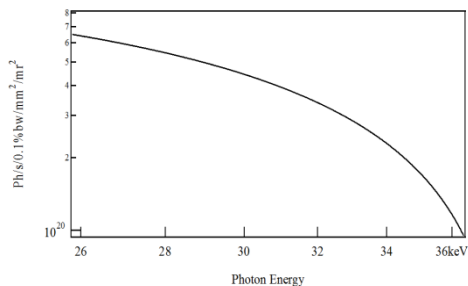


Fig. 8: Tuning curve for ESRF

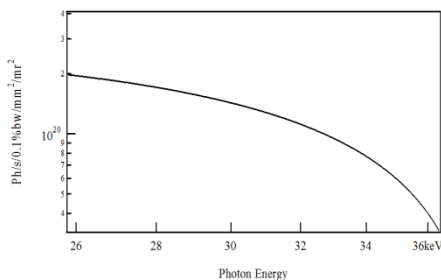


Fig. 9: Tuning curve for min input at CEBAF

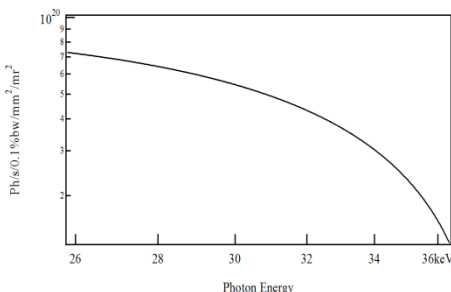


Fig. 10: Tuning curve for min x-ray spot at CEBAF

SUMMARY

From the calculations shown above, we learn that comparable x-ray brilliance and higher flux density (than that of ESRF) can be achieved at CEBAF with waist-at-target scheme despite of the extreme low average beam current. The improvement of flux density at CEBAF (about factor of 2) with optimal focusing is consistent with what expected from the theory. Intensity distributions confirm the benefit of optimal focusing.

The author would like to thank M. Minty for her support of this work.

REFERENCES

- [1] C. Leemann, D. Douglas, et al, "The Continuous Electron Beam Accelerator Facility: CEBAF at the Jefferson Laboratory". Annual Review of Nuclear and Particle Science **51**(1): 413-450.
- [2] A. Bogacz, et al, "Sub-picosecond X-rays from CEBAF at Jefferson Lab", AIP Conference Proceedings, 705, 29 (2004).
- [3] D. H. Bilderback, et al, "Review of third and next generation synchrotron light sources", J. Phys. B(2005): At. Mol. Opt. Phys. 38 S773
- [4] L. Harwood, "Upgrading CEBAF to 12 GeV", Proceedings of LINAC2002, Gyeongju, Korea, p620-622.
- [5] R. Talman, "Exploiting linac flexibility to produce a superior X-ray facility", Proceedings of PAC09, Vancouver, Canada, p1138-1140.
- [6] R. Talman, "How best to produce hard monochromatic x-rays from an electron beam", Unpublished.
- [7] O. Chubar, P. Elleaume, S. Kuznetsov and A. Snigirev, "Physical optics computer code optimized for synchrotron radiation", Proc. SPIE Int. Soc. Opt. Eng. **4769** (2002), p. 145